J Therm Anal Calorim (2010) 99:621–629
DOI 10.1007/s10973-009-0285-z

Thermomechanical characterization of PVDF and P(VDF-TrFE) blends containing corn starch and natural rubber

R. D. Simoes · M. A. Rodriguez-Perez ·
J. A. de Saja · C. J. L. Constantino

Received: 29 April 2009 / Accepted: 30 June 2009 / Published online: 6 August 2009
© Akadémiai Kiadó, Budapest, Hungary 2009

Abstract Films of poly(vinylidene fluoride), PVDF, and poly(vinylidene fluoride – trifluoroethylene), P(VDF-TrFE), containing corn starch and latex of natural rubber as additives were produced by compressing/annealing forming blends visioning applications as biomaterials. Therefore, considering the possible applications of these blends, a basic characterization has been carried out targeting to infer on their thermomechanical properties. The polymer films (PVDF and P(VDF-TrFE)) with different percentage of additives were characterized using scanning electron microscopy (SEM), Fourier transform infrared spectroscopy (FTIR), thermogravimetry (TG), differential scanning calorimetry (DSC), and dynamical-mechanical analysis (DMA). The compressing/annealing process allowed discarding the necessity of using the solvents to dissolve either PVDF or P(VDF-TrFE), which are usually toxic to human. The results showed that the polymers do not interact chemically with the additives with the blends showing high thermal stability and elasticity modulus at the same order of magnitude of the bone, for instance. The SEM imaged revealed that the blends present morphological structures of typical physical mixtures where each material can be identified within the blends.

Keywords PVDF · P(VDF-TrFE) · Films · Blends · Thermomechanical properties

Introduction

Polymeric blends have been studied for making possible significant modifications in the traditional properties of synthetic polymers [1, 2]. For instance, the poly(vinylidene fluoride), PVDF, and its copolymer poly(vinylidene fluoride-trifluoroethylene), P(VDF-TrFE), attract scientific and technological interest due to their mechanical and electrical properties where the piezoelectricity makes them a transducer in several application [3–5].

The PVDF crystalline phases are known as α (nonpolar), β (polar), γ (polar), and δ (α polar). The α phase is the most common, since the material normally is crystallized in this phase while the β phase is usually the most desirable due to its pyre and piezoelectric properties [6]. However, the crystallization of the PVDF in the β phase does not occur directly, in normal conditions, from the melted material [6, 7]. More recently, the PVDF as a biocompatible material has been investigated in monofilament vascular suture, fabrication of mechanically active tissue engineering scaffolds, bony restoration and bony filling, substrates to enhance nerve-fiber outgrowth invitro, and enzyme immobilization [8–13].

The P(VDF-TrFE) that can be synthesized with different TrFE molar ratios is crystallized directly in the ferroelectric phase, which is polar and similar to the β phase of PVDF, and the degree of crystallinity depends on the thermal treatment [14, 15]. Besides, its phase transition from ferroelectric to paraelectric occurs below the melting point and, due to polar nature of the material, also presents

R. D. Simoes · C. J. L. Constantino (✉)
DFQB, Faculdade de Ciências e Tecnologia, UNESP,
19060-900 Presidente Prudente, SP, Brazil
e-mail: case@fct.unesp.br

R. D. Simoes · M. A. Rodriguez-Perez · J. A. de Saja
Science Faculty, Condensed Matter Physics Department,
Cellular Materials Group (CellMat), University of Valladolid,
47011 Valladolid, Spain

M. A. Rodriguez-Perez · J. A. de Saja
Unidad Asociada Instituto Estructura de la Materia (CSIC),
Madrid, Spain

polarization of 2nd order, therefore, non-linear optical properties [16]. In terms of application as biomaterial, the P(VDF-TrFE) has been investigated as a bioactive material for enhancing bone regeneration and vascular prostheses [10, 17, 18].

The natural rubber latex (NR) obtained from the *Hevea brasiliensis* trees [19] is essentially composed by poly cis-1,4-isoprene, besides proteins, amino acids, carbohydrates, lipids, and nucleic acids [19, 20]. It presents interesting properties such as elasticity, abrasion resistance, electrical insulating, and impermeability to gases and liquids [20]. More recently, its biological activity as angiogenesis inducer has been investigated [21–23]. Corn starch is a polysaccharide of glucose, insoluble in cold water; but capable to hold water, being constituted by two types of polymeric chains: amylose, which is linear, and amylopectin, which is branched [24, 25]. Its viscoelastic properties under physiological conditions and substrate for bone cells or proteins have been studied [26, 27].

In this work, the main goal is to study the thermomechanical properties of blends containing PVDF or P(VDF-TrFE) with corn starch and NR as additives whose molecular structures are given in Fig. 1. The materials are processed by compressing under annealing until reaching the melting point of the polymeric matrix to form films targeting to exploit them as biomaterials. This process is chosen to avoid using any kind of solvents, which are usually toxics to human, while the NR presents elastomeric properties that allow one to tune the thermomechanical properties of the blends and the starch can be absorbed by the human body forming porous, besides both additives are biocompatible and biodegradable materials.

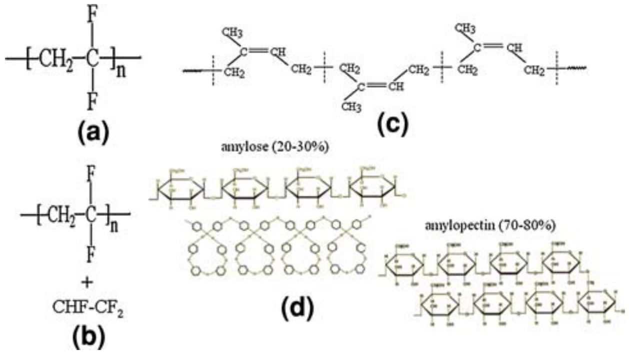

Fig. 1 Molecular structures of **a** PVDF mere unit, **b** P(VDF-TrFE) mere unit, **c** poly cis-1,4-isoprene segment, and **d** amylose and amylopectin segments

Experimental procedure

The PVDF Florafon F4000 HD was purchased from Atochem in the form of pellets and grounded in a cryogenic grinder producing a powder with particles of ca. 30 μm in diameter. The copolymer P(VDF-TrFE) 72/28 wt% was purchased from Piezotech in the powder form. The latex of NR, collected from different trees of *Hevea brasiliensis*, clones RRIM-600 (RRIM—Rubber Research Institute of Malaysia), was supplied by Prof. Dr. A. E. Job. The stabilization of the latex was made using a commercial solution of NH_4OH (4.7 mL of NH_4OH for 100 mL of latex). The corn starch was supplied by Prof. Dr. A. J. F. Carvalho. Nine samples were produced mixing the polymer (PVDF or P(VDF-TrFE)) with the additive (NR or starch or both). Table 1 presents the amount of each material used and their mass % in relation to the blend total mass. In the case of NR the % is calculated taking into account that the latex used contains ca 40% in mass of NR (called dry rubber as well) determined by TG [28]. Both binary and ternary blends were produced.

The mixing between the polymer and the additive is carried out manually during ca 20 min using a pestle. Then, the polymer/additive mixture obtained is placed in an aluminum frame leading to the fabrication of films with thickness of 0.4 mm. The compression of this system was made in a hydraulic press Forte Charlott, which is coupled

Table 1 Mass % of each material in relation to the blend total mass and the names to specify each sample

Film compositions	% in mass of each material in relation to the total mass of the blend	Film names
PVDF		PVDF
P(VDF-TrFE)		P(VDF-TrFE)
Natural rubber latex		NR
2.0 g PVDF/1.0 g starch	66.6% PVDF/33.3% starch	PVDF/starch
2.0 g P(VDF-TrFE)/1.0 g starch	66.6% P(VDF-TrFE)/33.3% starch	P(VDF-TrFE)/starch
2.0 g PVDF/1.0 mL latex	83.7% PVDF/16.3% NR	PVDF/NR
2.0 g P(VDF-TrFE)/1.0 mL latex	83.7% P(VDF-TrFE)/16.3% NR	P(VDF-TrFE)/NR
3.0 g PVDF/1.0 g starch/1.0 mL latex	61.2% PVDF/29.2% starch/9.6% NR	PVDF/starch/NR
3.0 g P(VDF-TrFE)/1.0 g starch/1.0 mL latex	61.2% P(VDF-TrFE)/29.2% starch/9.6% NR	P(VDF-TrFE)/starch/NR

Table 2 Static and dynamic forces for DMA curves of the three point model

Materials	Static force/mN	Dynamic force/mN
PVDF	480	400
P(VDF-TrFE)	400	350
NR	10	7
PVDF/starch	360	300
P(VDF-TrFE)/starch	600	500
PVDF/NR	240	200
P(VDF-TrFE)/NR	360	300
PVDF/starch/NR	360	300
P(VDF-TrFE)/starch/NR	360	300

to a temperature controller Contempcom model PXV. In the case of PVDF blends the temperature was 180 °C and in the case of P(VDF-TrFE) blends the temperature was 165 °C, which were chosen to ensure a complete melting of the polymers.

The SEM images were recorded using a JEOL equipment model JSM-820 (3 and 20 kV). Samples were fractured at low temperatures and coated with gold before SEM characterization. FTIR measurements were carried out in a Bruker spectrometer model Tensor 27 using the ATR mode (not polarized), 64 scans, and 4 cm^{-1} spectral resolution. The thermogravimetry (TG) was carried out using a Mettler TGA/SDTA 851^e equipment for samples with ca. 12.0 mg from 50 to 850 °C at 10 °C min^{-1} in N_2 atmosphere and from 850 to 950 °C in air. Differential scanning calorimetry (DSC) was performed using a Mettler DSC30 equipment for samples with ca. 5.0 mg from −120 to 200 °C at 10 °C min^{-1} and using N_2. Dynamical mechanical analysis (DMA) was performed in three point bending using a Perkin Elmer DMA^7 from −40 to 150 °C at 5 °C min^{-1}, frequency of 1 Hz, and using N_2. The sample size was 5.0 mm × 20.0 mm and thickness of 0.4 mm. The static and dynamic forces are given in Table 2. All the experiments were performed at very low static and dynamic strains (<1%). The DMA measurements were repeated at least three times for all the films. The results presented are the average of all curves.

Results and discussion

Infrared absorption (FTIR)

The FTIR technique was applied with both targets to determine the crystalline phase of the polymers in the films and to investigate the nature of the interaction polymer/additive. Figure 2 shows the FTIR spectra recorded for the films of PVDF, PVDF/NR, PVDF/starch, and NR and the starch powder while Fig. 3 shows the FTIR spectra recorded for the films of P(VDF-TrFE), P(VDF-TrFE)/NR, P(VDF-TrFE)/starch, and NR and starch powder. The PVDF FTIR spectrum in Fig. 2 shows that the PVDF is in the α phase with the main bands given in Table 3 [29] and the P(VDF-TrFE) FTIR spectrum in Fig. 3 shows that the P(VDF-TrFE) is in the ferroelectric phase with the main bands presented in Table 3 [30]. Besides, the FTIR spectra of the films containing PVDF/NR and PVDF/starch in Fig. 2 and P(VDF-TrFE)/NR and P(VDF-TrFE)/starch in Fig. 3 are totally dominated by the polymers. This indicates that there is not a strong chemical interaction polymer/additive, modifying the chemical nature of a significant amount of the system. If that was the case, then the FTIR spectra of the blends should present significant changes such as new band(s), displacement in frequency and/or variation in the relative intensity of the band(s) involved in the chemical interaction [31]. Therefore, the properties of the bends will depend on the interfacial adhesion or compatibility between phases. This has been analyzed by using SEM in the next section.

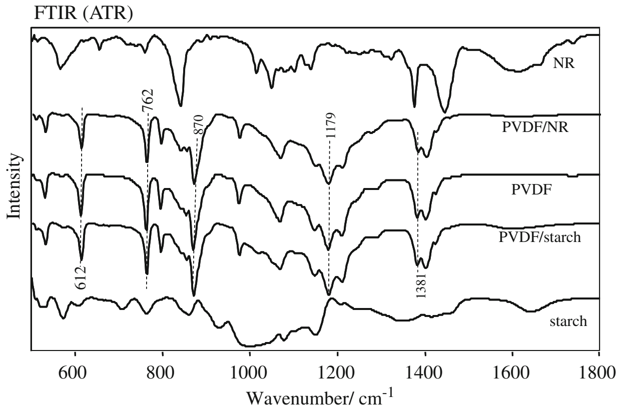

Fig. 2 FTIR spectra starch powder and films of PVDF, NR, PVDF/starch, and PVDF/NR

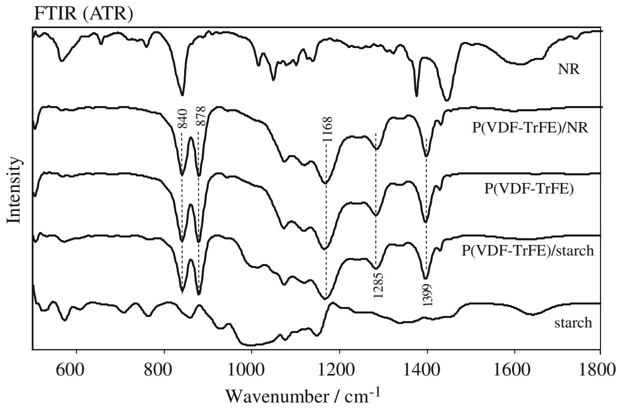

Fig. 3 FTIR spectra of starch powder and films of P(VDF-TrFE), NR, P(VDF-TrFE)/starch, and P(VDF-TrFE)/NR

Table 3 FTIR bands in cm^{-1} and assignments for the films of PVDF and P(VDF-TrFE)

PVDF		P(VDF-TrFE)	
Band/cm^{-1}	Assignments	Band/cm^{-1}	Assignments
612	CF_2 δ; CCC δ	840	CF_2 ν_s; CC ν_s
762	CF_2 δ; CCC δ	878	CH_2 r; CF_2 ν_a; CF_2 r
870	CC ν_s; CCC δ	1168	CF_2 ν_a; CF_2 r
1179	CF_2 ν_a; CH_2 w	1285	CH_2 ν_s; CC ν_s; CCC δ
1381	CH_2 δ; CH_2 w	1399	CH_2 w; CC ν_s

ν_s Symmetric stretching, ν_a antisymmetric stretching, δ scissoring, w wagging, r rocking

Scanning electron microscopy (SEM)

The morphology of the blends forming compressed films was investigated through SEM. Figure 4a–f show the SEM images with different magnification of the transversal section (across the volume) of compressed films formed either by blends (PVDF/starch (4a), P(VDF-TrFE)/starch (4b), PVDF/NR (4c), P(VDF-TrFE)/NR (4d), PVDF/starch/NR (4e), and P(VDF-TrFE)/starch/NR (4f)). The compressed films of the blends present morphological structures of a typically physical mixture where the structure of each material can be identified when in the blend. Comparing the morphology of the blends PVDF/starch and P(VDF-TrFE)/starch, Fig. 4a and b, it can be inferred that a better physical adhesion occurs for the film P(VDF-TrFE)/starch, which must be related to the polarity introduced by the trifluoroethylene groups.

Comparing the morphology of the blends PVDF/NR and P(VDF-TrFE)/NR, Fig. 4c and d, it is observed that both phases can be distinguished with the NR presenting domains of around 20 microns and a good compatibility with both polymers. However, a good physical adhesion is seen for both blends. In Fig. 4e and f are presented the SEM images of the blends PVDF/starch/NR and P(VDF-TrFE)/starch/NR. Curiously, the starch particles, that are well defined in the blends with PVDF and P(VDF-TrFE), are barely observed when the NR is present (Fig. 4e shows a spot hardly found, where the starch particle can be observed). Since the starch is not soluble in the NR at the conditions worked here, the particles might be involved by the NR. Therefore, it seems that the NR phase is acting as a compatibilizer between PVDF and starch, improving the interfacial adhesion between phases.

Thermogravimetry (TG)

The measurements of TG were carried out with the objective to verify the thermal stability of the films, since to be applied as biomaterials it is necessary to be highly steady not only in the temperature of the human body, but mainly in higher intervals of temperature, which involve sterilization processes. Figures 5, 6, and 7 show the curves of TG recorded with 10 °C min^{-1} for the starch powder and for the films of PVDF, P(VDF-TrFE), NR, PVDF/starch, P(VDF-TrFE)/starch, PVDF/NR, P(VDF-TrFE)/NR, PVDF/starch/NR, P(VDF-TrFE)/starch/NR. The DTG curves are given in the insets of Figs. 5, 6, and 7.

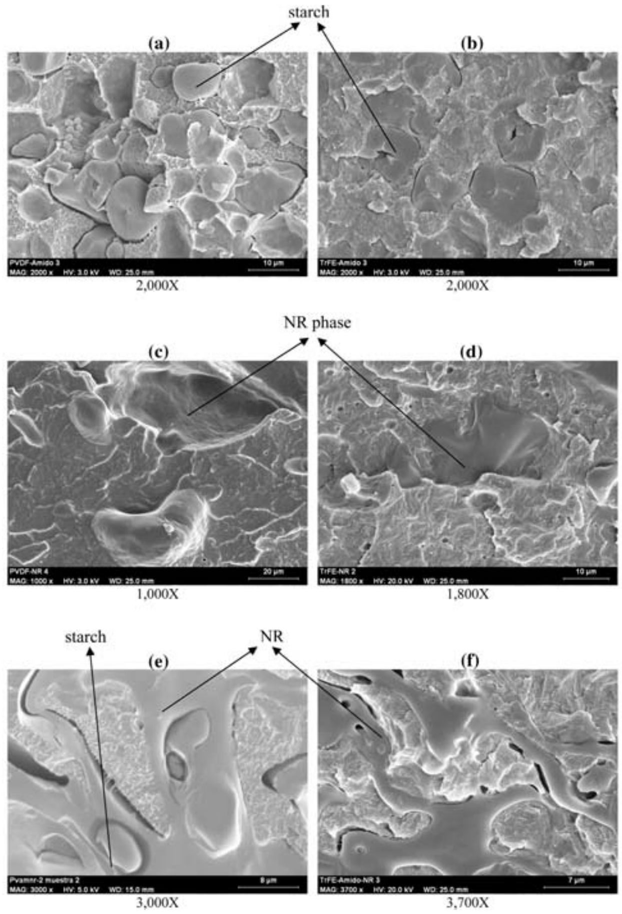

Fig. 4 SEM of the transversal section for the blends forming compressed films containing **a** PVDF/starch; **b** P(VDF-TrFE)/starch; **c** PVDF/NR; **d** P(VDF-TrFE)/NR; **e** PVDF/starch/NR, and **f** P(VDF-TrFE)/starch/NR

A good thermal stability can be observed for PVDF, P(VDF-TrFE), starch, NR, and the respective blends as well [20, 28, 32]. The thermal degradation due to annealing process under nitrogen atmosphere starts at ca. 450 °C for both PVDF and P(VDF-TrFE) films, at 300 °C for starch, and at 200 °C for NR. In the case of the blends it starts at ca. 300 °C for PVDF/starch, P(VDF-TrFE)/starch, PVDF/starch/NR, and P(VDF-TrFE)/starch/NR, and at ca. 360 °C for NR/PVDF. These results indicate that all the blends are suitable materials in terms of the application desired considering the physical and chemical stabilities with temperature. In general way, with exception of the losses of

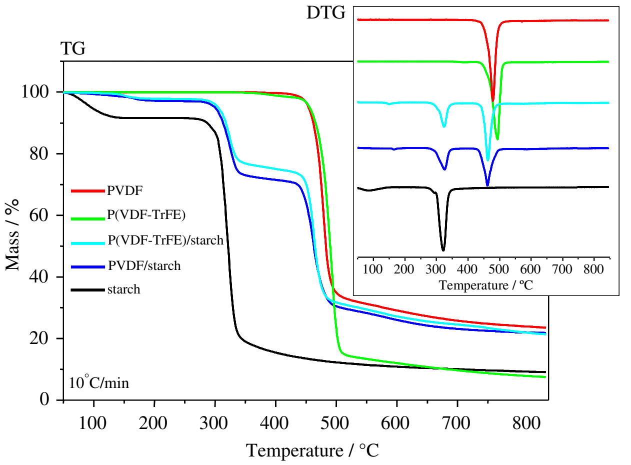

Fig. 5 TG curves for the starch powder and films of PVDF, P(VDF-TrFE), PVDF/starch, and P(VDF-TrFE)/starch. The inset shows the DTG curves

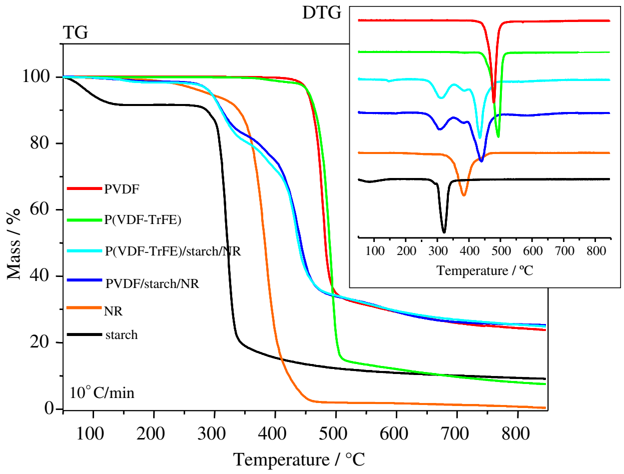

Fig. 7 TG for the starch powder and films of PVDF, P(VDF-TrFE), NR, PVDF/starch/NR, and P(VDF-TrFE)/starch/NR. The inset shows the DTG curves

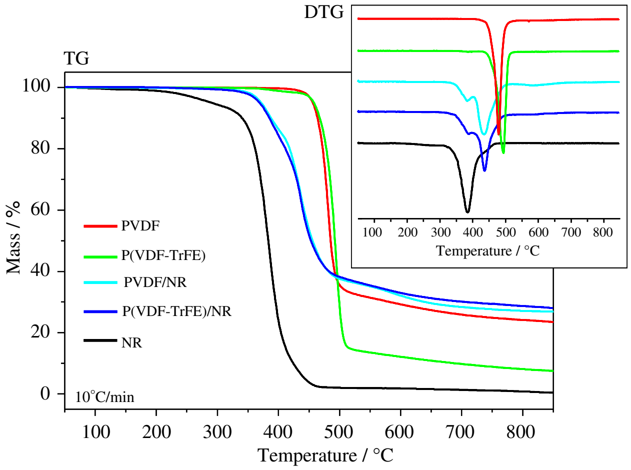

Fig. 6 TG curves for the films of PVDF, P(VDF-TrFE), NR, PVDF/NR, and P(VDF-TrFE)/NR. The inset shows the DTG curves

humidity, about 9% for the starch and 5% for the NR, the TG curves for the neat materials (starch, PVDF, P(VDF-TrFE), and NR) presented only one inflection related to the mass loss being ca. 74% for the starch, 67% for the PVDF, 91% for P(VDF-TrFE), and 95% for the NR with a residual mass around 17% for the starch, 33% for the PVDF, and 9% for the P(VDF-TrFE).

The TG curve for the films of PVDF/starch in Fig. 5 presents a residual mass of ca. 23%, being 20% related to PVDF and 3% to starch, and three inflections related to the mass loss. The first inflection at 150 °C corresponds to approximately 2% and is attributed to the humidity in the starch. The second inflection at ca. 300 °C corresponds to approximately 21% and is assigned to the degradation of the starch and the third inflection around 400 °C and mass loss of ca. 44% is attributed to the PVDF. The TG curve for P(VDF-TrFE)/starch is similar to those of the blend PVDF/starch, where at ca. 300 °C there is a mass loss around 25% (starch) and at ca. 400 °C there is a mass loss of approximately 42% (P(VDF-TrFE)) with a residual mass of ca. 23%.

The TG curves for the films of PVDF/NR and P(VDF-TrFE)/NR in Fig. 6 are very similar showing a residual mass of approximately 33%. They also present two small inflections related to the mass loss of the polymers. The first inflection around 380 °C with a mass loss of ca. 15% is related to the burning of the NR while the second inflection around 440 °C with a mass loss of ca. 50% is attributed to the thermal degradation of the polymeric matrix, that is, PVDF or P(VDF-TrFE).

The TG curves for the films of PVDF/starch/NR and P(VDF-TrFE)/starch/NR given in Fig. 7, besides presenting a residual mass of approximately 25%, four inflections related to the mass loss are observed. The first one at ca. 150 °C of approximately 6% is attributed to the humidity of the starch. The second at ca. 300 °C and mass loss around 13% corresponds to the thermal degradation of the starch. The third at ca. 350 °C and 7% of mass loss is related to the burning of the NR while the fourth around 400 °C and mass loss of ca. 44% is assigned to the polymeric matrix (PVDF or P(VDF-TrFE)).

It is observed for all the blends a significant % of residual mass even at high temperatures (900 °C). In general, the PVDF residual mass is very dependent on the processing methods. The presence of additives introduced during commercial polymer processing, such as lubricants and plasticizers, or the presence of solvent molecules and/or radicals remaining in the samples prepared in the labs, and reactions of the macromolecules with small molecules and/or radicals that exist in the polymer are responsible for high values of residual mass [33]. Particularly, in the case of PVDF used in this work, it presents intrinsically a high % of residual mass independent of how the samples were prepared in the lab. For instance, the TG of the PVDF pellet bought from ATOCHEM and used in this work presents ca. 30% of residual mass as reported by Campos et al. [34]. In terms of the P(VDF-TrFE), for the blend containing P(VDF-TrFE)/starch, both pure materials present a residual mass around 10% while the residual mass of the blend is around 25%. In terms of a physical explanation for that, it could be speculated that a better mixture among the materials could lead to a better thermal stability, which is consistent with SEM results. The same can be said for the P(VDF-TrFE)/NR blends.

Differential scanning calorimetry (DSC)

The identification of the crystalline phases of the PVDF and the P(VDF-TrFE), the glass transition temperature (T_g), and the melting temperature (T_m) as well were investigated using DSC. In Figs. 8, 9, and 10 are presented the measurements of DSC for the starch powder and for the films of PVDF, P(VDF-TrFE), NR, PVDF/starch, P(VDF-TrFE)/starch, PVDF/NR, P(VDF-TrFE)/NR, PVDF/starch/NR, and P(VDF-TrFE)/starch/NR recorded with 10 °C min^{-1} between −120 and 200 °C.

In general way, the curves of DSC for the blends follow the behavior of the polymers (PVDF or P(VDF-TrFE)) considering the interval of temperature, which is in agreement with the lack of chemical interaction between the materials as shown by FTIR. The DSC curves for the neat PVDF and PVDF blends presented endothermic peaks (↓) at ca. 167 °C related to the melting of the PVDF α-phase [7]. A similar trend was found for the DSC curves of the P(VDF-TrFE) and P(VDF-TrFE) blends. In this case two well-defined endothermic peaks (↓) were observed. The first one at 132 °C corresponds to the ferroelectric-paraelectric transition (Curie transition) and the second one to the melting of the P(VDF-TrFE) paraelectric phase at 148 °C [32]. It is important to notice that the manufacturing process of the sample and its thermal history can strongly influence the temperature of crystalline melting point of both PVDF and P(VDF-TrFE) [7]. The certainty of the assignments given to the crystalline phase in this case came from FTIR measurements. In terms of the NR, the DSC curves shows a base-line difference at ca. −70 °C, which corresponds to its T_g [20]. Endothermic peak of starch is attributable to vaporization of bound water restrained by hydroxyl group of starch.

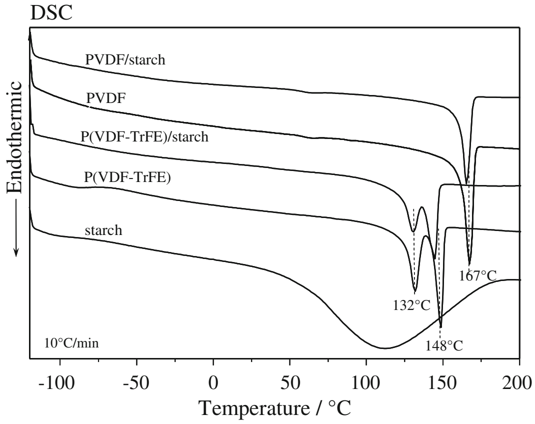

Fig. 8 DSC curves for the starch powder and films of PVDF, P(VDF-TrFE), PVDF/starch, and P(VDF-TrFE)/starch

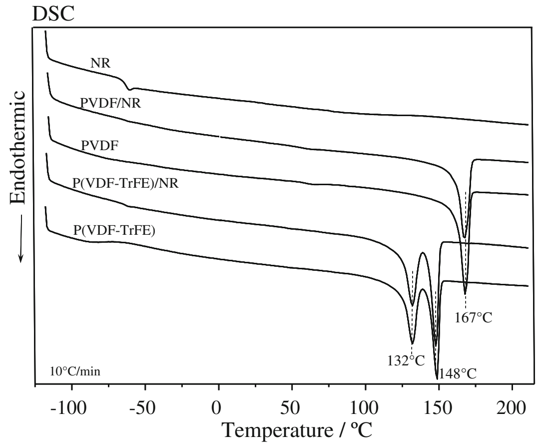

Fig. 9 DSC curves for the films of PVDF, P(VDF-TrFE), NR, PVDF/NR, and P(VDF-TrFE)/NR

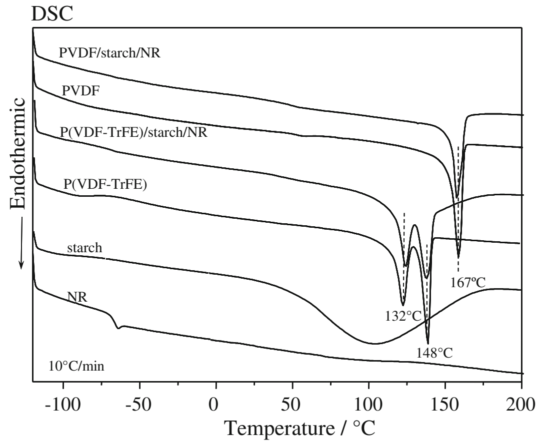

Fig. 10 DSC curves for the starch powder and films of PVDF, P(VDF-TrFE), NR, PVDF/starch/NR, and P(VDF-TrFE)/starch/NR

Dynamical mechanical analysis (DMA)

The DMA measurements were carried out with the objective to investigate the elasticity or storage modulus (E') of

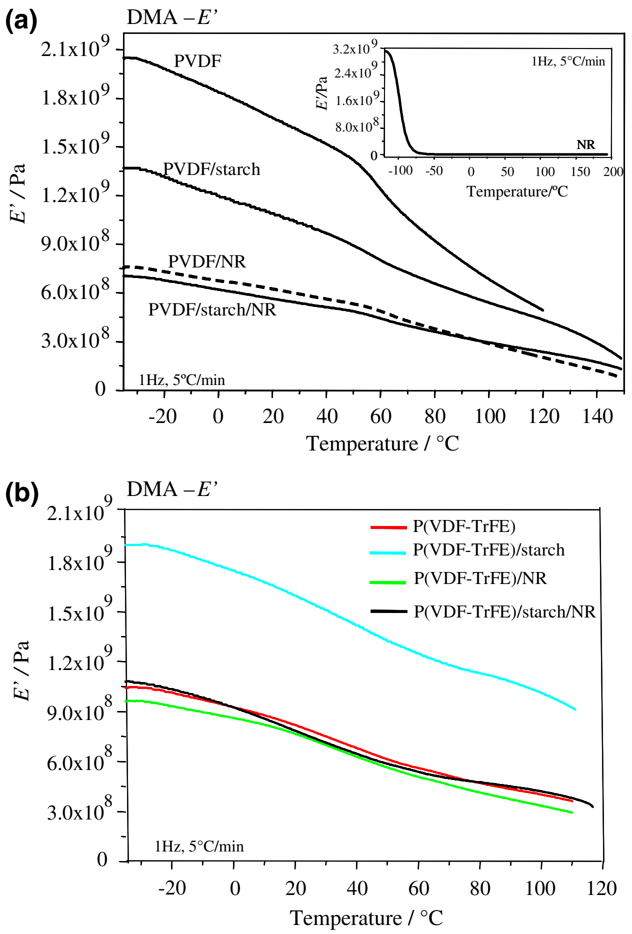

Fig. 11 **a** E' for the films of PVDF, PVDF/starch, PVDF/NR, and PVDF/starch/NR (NR in the inset). **b** E' for the films of P(VDF-TrFE), P(VDF-TrFE)/starch, P(VDF-TrFE)/NR, and P(VDF-TrFE)/starch/NR

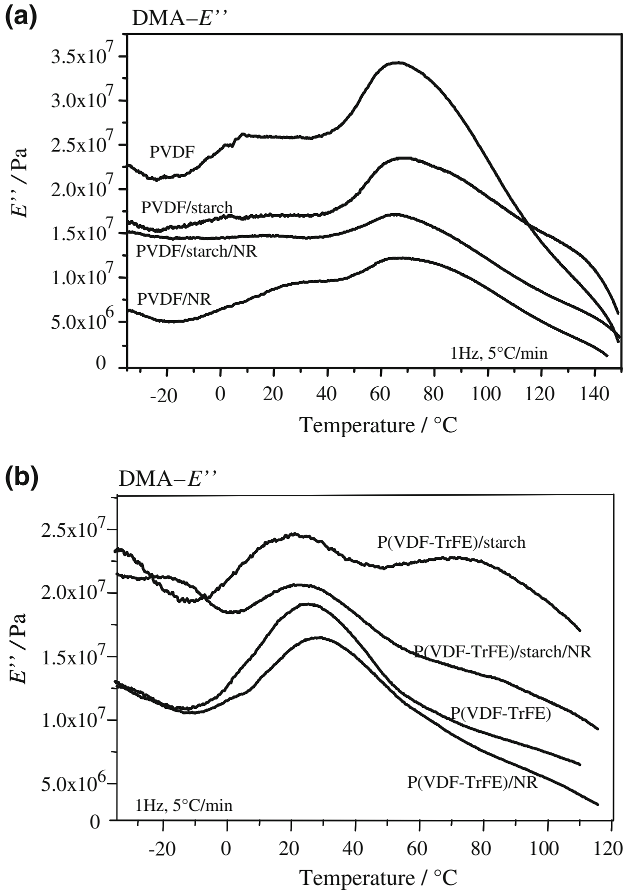

Fig. 12 **a** E'' for the films of PVDF, PVDF/starch, PVDF/NR, and PVDF/starch/NR. **b** E'' for the films of P(VDF-TrFE), P(VDF-TrFE)/starch, P(VDF-TrFE)/NR, and P(VDF-TrFE)/starch/NR

the blends at different temperatures and their T_g through tan δ curves (E''/E', E'': loss modulus). Figure 11a presents the values of E' (elasticity modulus) for the films of PVDF, PVDF/starch, PVDF/NR, and PVDF/starch/NR and Fig. 11b presents the values of E' for the films of P(VDF-TrFE), P(VDF-TrFE)/starch, P(VDF-TrFE)/NR, and P(VDF-TrFE)/starch/NR. The inset in Fig. 11a shows the E' values for the NR film. In terms of E', it can be seen that the starch and NR leads to PVDF blends less stiff (lower E' values) with the NR playing a more significant role. On the other hand, considering the P(VDF-TrFE), the blends containing NR (P(VDF-TrFE)/NR and P(VDF-TrFE)/starch/NR) present close E' values in relation to the neat P(VDF-TrFE), which is less stiff itself than the PVDF. However, the presence of starch in the P(VDF-TrFE)/starch blend makes the film stiffer. This behavior can be been explained by a better interfacial adhesion between starch and P(VDF-TrFE) based on scanning electron microscopy (SEM—results not shown). Besides, it is important to notice that all the blends can reach E' values in the order of magnitude of the bone [35].

Figure 12a and b present the curves of E'' recorded at 5 °C min^{-1} and 1 Hz for the films containing PVDF and P(VDF-TrFE), respectively. In the literature [36, 37], the E'' curves for the PVDF can present up to four relaxations named γ (−70 °C) attributed to the amorphous phase (rotation movements of the chains), β (−40 °C) corresponding to the glass transition, γ' (50 °C) attributed to the amorphous phase (folding movements), and α (100 °C), which it is an opened question, being attributed to motions in the amorphous phase or in the crystalline phase. In our case, two relaxations were observed in the E'' for PVDF based materials, the first one around at approximately 20 °C and the second one at about 70 °C. These relaxations appeared for all the materials, neat PVDF and its blends at similar temperatures, indicating again that no interactions exist between the materials in the blends. In the case of P(VDF-TrFE) two relaxations (tan δ) are usually observed in the literature, one at ca. −25 °C attributed to segmental motions in the amorphous region and other at ca. 30 °C related to segmental motions in the crystalline fraction [32]. Both relaxations were observed in the E'' curves for the materials based on this polymer.

Conclusions

Films of PVDF and P(VDF-TrFE) containing starch and latex of natural rubber (NR) as additives were possible to be fabricated avoiding using any solvent, which is an important issue considering their applications as biomaterials. The films were producing by compressing/annealing mixtures of PVDF, starch, and NR or P(VDF-TrFE), starch, and NR at 180 and 165 °C, respectively, which are slightly above the melting point of the polymers. The FTIR showed that both PVDF and P(VDF-TrFE) do not interact chemically with the additives forming polymeric blends. Besides, SEM images revealed that the materials within the blends form separated phases with the interfacial adhesion between two phases depending on the materials that form the blends. For instance, the blends whose matrix is formed by P(VDF-TrFE) allow a better interfacial adhesion. The TG measurements showed that the blends are thermally stable up to 300 °C, which is fair enough considering that sterilization is the hardest thermal treatment that these films might be submitted when applied as biomaterials. Besides, the DSC curves revealed that the phase transition of the blends follow the polymers, being at 167 °C for PVDF, assigned to the melting point, and at 132 and 148 °C for P(VDF-TrFE), which correspond to the transition from ferroelectric to paraelectric phase and melting point, respectively. In terms of mechanical properties, the elasticity modulus (E') is within 200 and 2,000 MPa for a temperature range between −30 and 140 °C. Besides, the starch and the NR play different roles on the E' values of the polymers. The E' values of the PVDF blends are lower than the PVDF itself while the E' value of the P(VDF-TrFE) blend containing starch is higher than the P(VDF-TrFE) itself, which is not significantly affected by the presence of NR.

Acknowledgements FAPESP and CAPES (process 118/06) from Brazil and Fundación Carolina and MICINN (PHB2005-0057-PC) from Spain for the financial support.

References

1. Wang Y, Wang J, Wang F, Li S, Xiao J. PVDF based all-organic composite with high dielectric constant. Polym Bull. 2008;60:647–55.
2. Ciesinska W, Zielinski J, Brzozowska T. Thermal treatment of pitch-polymer blends. J Therm Anal Calorim. 2009;95:193–6.
3. Molenda M, Dziembaj R, Piwowarska Z, Drozdek M. A new method of coating powdered supports with conductive carbon films. J Therm Anal Calorim. 2007;88:503–6.
4. Chinaglia DL, Schmidt TF, Santos LF, Balogh DT, Oliveira ON Jr, Faria RM. Fabrication of novel light-emitting devices based on green-phosphor/conductive-polymer composites. Philos Mag Lett. 2007;87:403–8.
5. Ito A, Tanaka K, Kawaji H, Atake T, Ando N, Hato Y. Magnetic phase transition of $Li_{0.75}CoO_2$ compared with $LiCoO_2$ and $Li_{0.5}CoO_2$. J Therm Anal Calorim. 2008;92:399–401.
6. Nalwa HS. Ferroelectric polymers: chemistry, physics and applications. New York: Marcel Dekker; 1995.
7. Gregorio R Jr, Cestari M. Effect of crystallization temperature on the crystalline phase content and morphology of poly(vinylidene Fluoride). J Polym Sci. 1994;32:859–70.
8. Tabary N, Lepretre S, Boschin F, Blanchemain N, Neut C, Delcourt-Debruyne E, et al. Functionalization of PVDF membranes with carbohydrate derivates for the controlled delivery of chlorhexidin. Biomol Eng. 2007;24:472–6.
9. Gallego-Perez D, Ferrell N, Hansford DJ. Fabrication of piezoelectric Polyvinylidene Fluoride (PVDF) microstructures by soft lithography for tissue engineering and cell biology applications. In: MRS Spring Meeting San Francisco, California. 2007. http://www.mrs.org/s_mrs/sec_subscribe.asp?CID=8775&DID=201955&action=detail Accessed 12 June 2009.
10. Callegari B, Belangero WD. Análise da interface formada entre o polifluoreto de vinilideno (piezelétrico e não piezelétrico) e o tecido ósseo de ratos. Acta Ortopedica Brasileira. 2004;12:160–6.
11. Laroche G, Marois Y, Guidoin R, King MW, Martin L, How T, et al. Polyvinylidene fluoride (PVDF) as a biomaterial: from polymeric raw material to monofilament vascular suture. J Biomed Mater Res. 1995;29:1525–36.
12. Valentini RF, Vargo TG, Gardella JA, Aebischer P. Electrically charged polymeric substrates enhance nerve fibre outgrowth *In vitro*. Biomaterials. 1992;13:183–90.
13. Aoshima R, Kanda Y, Takada A, Yamashita A. Sulfonated poly(vinylidene fluoride) as a biomaterial—immobilization of urokinase and biocompatibility. J Biomed Mater Res. 1982;16:289–99.
14. Fernandez MV, Suzuki A, Chiba A. Study of annealing effects on the structure of vinylidene fluoride-trifluoroethylene copolymers using WAXS and SAXS. Macromoleculares. 1987;20:1806–11.
15. Matsumoto A, Horie S, Yamada H, Matsushige K, Kuwajima S, Ishida K. Ferro- and piezoelectric properties of vinylidene fluoride oligomer thin film fabricated on flexible polymer film. Appl Phys Lett. 2007;90:290–6.
16. Ploss B, Ploss B. Dielectric nonlinearity of PVDF–TrFE copolymer. Polymer. 2000;41:6087–93.
17. Gimenes R, Zaghete MA, Bertolini MJ, Varela JA, Coelho LO, Silva NF. Composites PVDF-TrFE/BT used as bioactive membranes for enhancing bone regeneration (Proceedings Paper). Smart Structures and Materials 2004: Electroactive Polymer Actuators and Devices (EAPAD) 2004;5385:539–47.
18. Beloti MM, de Oliveira PT, Gimenes R, Zaghete MA, Bertolini MJ, Rosa AL. In vitro biocompatibility of a novel membrane of the composite poly(vinylidene-trifluoroethylene)/barium titanate. J Biomed Mater Res Part A. 2006;79A:282–8.
19. Agostini DLS, Constantino CJL, Job AE. Thermal degradation of both latex and latex cast film forming membranes combined TG/FTIR investigation. J Therm Anal Calorim. 2008;91:703–7.
20. de Oliveira LCS, de Arruda EJ, Favaro SP, da Costa RB, Gonçalves PS, Job AE. Evaluation of thermal behavior of latex membranes from genetically improved rubber tree (Hevea brasiliensis). Thermochim Acta. 2006;445:27–31.

21. Brandão ML, Coutinho Netto J, Thomazini JA, Lachat JJ, Muglia VF, Piccinato CE. Prótese vascular derivada do látex. Braz Vasc J. 2007;6:130–41.
22. Neves-Junior WFP, Ferreira M, Alves MCO, Graeff CFO, Mulato M, Coutinho-Netto J, et al. Influence of fabrication process on the final properties of natural-rubber latex tubes for vascular prosthesis. Braz J Phys. 2006;36:586–91.
23. Balabanian CACA, Coutinho-Netto J, Lamano-Carvalho TL, Lacerda SA, Brentegani LG. Biocompatibility of natural latex implanted into dental alveolus of ratos. J Oral Sci. 2006;48: 201–5.
24. Lacerda LG, da Carvalho Silva, Filho MA, Demiate IM, Bannach G, Ionashiro M, et al. Thermal behaviour of corn starch granules under action of fungal *α-amylase*. J Therm Anal Calorim. 2008; 93:445–9.
25. Gomes ME, Sikavitsas VI, Behravesh E, Reis RL, Mikos AG. Effect of flow perfusion on the osteogenic differentiation of bone marrow stromal cells cultured on starch-based three-dimensional scaffolds. J Biomed Mater Res Part A. 2003;67:87–95.
26. Alves CM, Yang Y, Carnes DL, Ong JL, Sylvia VL, Dean DD, et al. Modulating bone cells response onto starch-based biomaterials by surface plasma treatment and protein adsorption. Biomaterials. 2007;28:307–15.
27. Mano JF, Reis RL. Viscoelastic monitoring of starch-based biomaterials in simulated physiological conditions. Mater Sci Eng A. 2004;370:321–5.
28. Simoes RD, Job AE, Chinaglia DL, Zucolotto V, Camargo-Filho JC, Alves N, et al. Structural characterization of blends containing both PVDF and natural rubber latex. J Raman Spectrosc. 2005;36:1118–24.
29. Kobayashi M, Tashiro K, Tadokoro H. Molecular vibrations of three cristal forms of Poly(vinylidene Fluoride). Macromolecules. 1975;8:158–71.
30. Prabu AA, Lee JS, Kim KJ, Lee HS. Infrared spectroscopic studies on crystallization and Curie transition behavior of ultrathin films of P(VDF/TrFE) (72/28). Vib Spectrosc. 2006;41:1–13.
31. Piza MA, Constantino CJL, Venâncio EC, Mattoso LHC. Interaction mechanism of poly (o-ethoxyaniline) and collagen blends. Polymer. 2003;44:5663–70.
32. Sencadas V, Lanceros-Méndez S, Mano JF. Thermal characterization of a vinylidene fluoride-trifluorethylene (75–25) (%mol) copolymer film. J Non-Cryst Solids. 2006;352:5376–81.
33. Botelho G, Lanceros-Mendez S, Goncalves AM, Sencadas V, Rocha JG. Relationship between processing conditions, defects and thermal degradation of poly(vinylidene fluoride) in the b-phase. J Non-Cryst Solids. 2008;354:72–8.
34. Campos JSC, Ribeiro AA, Cardoso CX. Preparation and characterization of PVDF/$CaCO_3$ composites. Mater Sci Eng B. 2007; 136:123–8.
35. Basset CAL. Biochem Physiol Bone. New York: Academic Press; 1971.
36. Linares A, Costa JL. Tensile and dynamic mechanical behaviour of polymer blends based on PVDF. Eur Polym J. 1997;33:467–73.
37. Hatakeyama T, Liu Z, editors. Handbook of thermal analysis. New York: Wiley; 2000. p. 209.